ORIGINAL RESEARCH

Preparation of a nanoscale baohuoside I-phospholipid complex and determination of its absorption: in vivo and in vitro evaluations

Xin Jin[1,2]
Zhen-hai Zhang[1]
E Sun[1]
Qian Qian[1]
Xiao-bin Tan[1]
Xiao-bin Jia[1]

[1]Key Laboratory of New Drug Delivery System of Chinese Materia Medica, Jiangsu Provincial Academy of Chinese Medicine, [2]College of Pharmacy, Nanjing University of Chinese Medicine, Nanjing, People's Republic of China

Background: Baohuoside I is a potential anticancer drug for a variety of malignancies and has been approved for in vitro use. However, baohuoside I has very poor oral absorption.

Methods: In the present study, we prepared baohuoside I-phospholipid complexes of different diameters and determined their physicochemical properties using transmission electron microscopy, ultraviolet spectroscopy, and differential scanning calorimetry. The in vitro absorption of baohuoside I and baohuoside I-phospholipid complexes of different sizes were compared using the Caco-2 cell culture model, and subsequently, the bioavailability of baohuosidel and its complexes were estimated in vivo.

Results: Compared with the large-sized phospholipid complexes, a nanoscale phospholipid complex improved the oral bioavailability of baohuoside I. In addition, our results suggest that the smaller the particle size, the faster the complexes crossed the Caco-2 monolayer and the faster they were resorbed after oral administration in rats. The relative oral bioavailability of a nanoscale size 81 ± 10 nm baohuoside I-phospholipid complex (area under the concentration-time curve $[AUC]_{0-\infty}$) was 342%, while that of baohuoside I and a 227.3 ± 65.2 µm baohuoside I-phospholipid complex was 165%.

Conclusion: We enhanced the oral bioavailability of baohuoside I by reducing the particle size of the phospholipid complex to the nanometer range, thereby improving its potential for clinical application.

Keywords: nanoscale phospholipid complex, Caco-2 cell monolayer, bioavailability, oral absorption

Introduction

Herba epimedii, a herbal medicine derived from the dried aerial part of *Epimedium sagittatum* Maxim, has been traditionally used in China as a tonic, an aphrodisiac, and an antirheumatic drug for many years. Baohuoside I (also known as icariside II, Figure 1) is the main active component of Herba epimedii,[1] and induces apoptosis in human PC-3 prostate cancer cells via a mitochondrial-dependent pathway and inhibits the growth of U266 multiple myeloma and human osteosarcoma cells.[2–4] However, the poor water and oil solubility of baohuoside I causes many difficulties in the development of intravenous preparations. In addition, poor aqueous solubility and low membrane permeability limits the use of baohuoside I as a treatment of human ailments.[5]

Therefore, improvement in the oral absorption of baohuoside I may play an important role in determining its future applications. Phospholipids are the main components of the cell membrane and aid in the absorption of drugs.[6] Therefore, phospholipid

Correspondence: Xiao-bin Jia
Key Laboratory of New Drug Delivery System of Chinese Materia Medica, Jiangsu Provincial Academy of Chinese Medicine, 100 Shizi Road, Nanjing, Jiangsu 210028, People's Republic of China
Tel +86 25 8560 8672
Fax +86 25 8563 7809
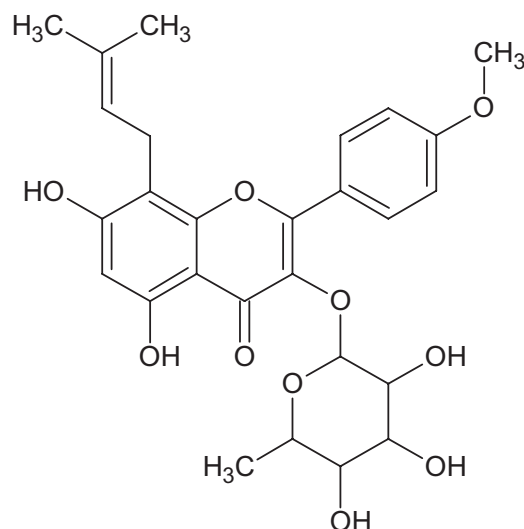Email xiaobinjia_nj@126.com

4907

Figure 1 Chemical structure of baohuoside I.

complexes are commonly used as carriers to increase the bioavailability of drugs,[7] and these complexes have been shown to improve gastrointestinal absorption, resulting in high serum drug concentrations. Phospholipids have extensive potential applications because of their ease of preparation.[8] The bioavailability of several natural drugs, such as curcumin,[9] clarithromycin,[10] and silymarin,[11] has been improved using phospholipid complexes.

Nanoparticles are particulate dispersions or solid particles ranging from 10 to 100 nm in size (in one dimension) and are being developed to improve drug bioavailability, abrogate treatment-induced drug resistance, and reduce nonspecific toxicity. Several recent studies have shown that nanomaterials can cross biological membranes and access cells, tissues, and organs that are normally inaccessible by large-sized particles. Therefore, the application of nanotechnology in the diagnosis and treatment of cancer has increased to overcome the serious side effects of anticancer agents, increasing their cytotoxic effects on normal cells.[12–15]

However, to the best of our knowledge, no studies have shown the influence of nanoscale phospholipid complexes on oral absorption. In the present study, high-pressure homogenization was used to prepare baohuoside I-phospholipid complexes of different sizes. The Caco-2 cell monolayer model was used to study the absorption of baohuoside I and its complexes in vitro because this model has been approved by the US Food and Drug Administration as an appropriate human intestinal absorption model to investigate drug absorption.[16,17] Furthermore, in vivo pharmacokinetic profiles

after oral administration were evaluated to determine the effect of the nanoscale phospholipid complex on absorption of baohuoside I.

Materials and methods
Instruments and materials

Cloned Caco-2 TC7 cells were a kind gift from Ming Hu of INSERM U178 (Houston, TX). Baohuoside I, carbamazepine, and genistein (all with purity > 98%) were provided by the Laboratory of Pharmaceutical Preparation (Jiangsu Provincial Academy of Chinese Medicine, China). Phospholipids and Hanks' balanced salt solution (powder form) were purchased from Sigma-Aldrich (St Louis, MO). Milli-Q water (Millipore, Bedford, MA) was used throughout the experiment. Acetonitrile and methanol were of chromatographic grade (Merck Company Inc, Whitehouse Station, NJ).

Animal experiments

Male Sprague-Dawley rats weighing 200–250 g were obtained from the SLEK Laboratory Animal Center of Shanghai (Shanghai, China). The animals were housed under standard conditions of temperature, humidity, and light. Food and water were provided ad libitum. The rats were fasted overnight before the day of the experiment. All animal care and experimental procedures were performed according to the Guiding Principles in the Use of Animals in Toxicology, as adopted in 1989, revised in 1999, and amended in 2008, by the Society of Toxicology.

Preparation of baohuoside I-phospholipid complex

The phospholipid complex was prepared by a reduction vaporization method using an anhydrous cosolvent. Briefly, baohuoside I and phospholipids (molar ratio 1:1) were codissolved in anhydrous ethanol by gentle agitation until a transparent solution was obtained, which was left standing for one day. After removing the solvent by reduced pressure distillation, the baohuoside I-phospholipid complex was obtained. The complex was then lapped and sieved to obtain the common baohuoside I-phospholipid complex. The baohuoside I-phospholipid complex was dispersed in distilled water and homogenized using a high-pressure homogenizer (Avestin Em-C3, Ottawa, Canada) to produce baohuoside I-phospholipid complexes of different sizes. The final dispersions of the phospholipid complex were stored at room temperature until required.

Characterization of nanometer-scale phospholipid complex

Particle size and zeta potential measurements

The particle size and zeta potential of the nanoscale phospholipid complex were determined by dynamic light scattering on a Zetasizer Nano-ZS (Malvern Instruments, Worcestershire, UK). The common phospholipid complex was determined using EyeTech (Ankersmid, Holland), and the morphology of the nanoscale phospholipid complex was evaluated using transmission electron microscopy (JEM-1200EX, Japan).

Ultraviolet spectroscopy

Baohuoside I and nanoscale 81 ± 10 nm baohuoside I-phospholipid complex were dissolved in ethanol and then analyzed using high-performance liquid chromatography and a diode array detector with the acquisition wavelength set in the range of 200–400 nm.

Differential scanning calorimetry

Samples were sealed in aluminum crimp cells and heated at a rate of 10°C per minute from 30°C to 450°C in a nitrogen atmosphere (DSC-60; Shimadzu, Tokyo, Japan). The maximum peak transition temperatures of the phospholipids, baohuoside I, physical mixtures of phospholipids and baohuoside I, and the nanoscale 81 ± 10 nm baohuoside I-phospholipid complexes were compared using a thermal analyzer (TA-60WS; Shimadzu).

Cell culture

The Caco-2 TC7 cells were cultured in the laboratories of Ming Hu at INSERM U178. The Caco-2 TC7 cell line is similar to the wild-type Caco-2 cell line, but is more stable during transportation because it is a cloned cell line.[18] The conditions for Caco-2 cell culture have been described previously.[19,20] For the transport assay, cells were seeded on Transwell® inserts in six-well Transwell plates, which have a surface area of 4.2 cm^2, at a density of 100,000 cells/cm^2 in growth medium (Dulbecco's modified Eagle's medium supplemented with 10% fetal bovine serum). The quality control criteria were based on previously published reports.[21,22] The culture medium was changed every 24 hours. Cells were cultured for at least 21 days at 37°C, 90% humidity, and 5% CO_2 before they were used for the transport studies between days 21 and 23.[23] Physiologically and morphologically well developed Caco-2 cell monolayers with transepithelial electrical resistance values greater than 300 Ωcm^2 were used for the experiments.

Transport experiments in Caco-2 cell cultures

Cell culture was performed as described previously.[19,21] Briefly, after the culture medium was aspirated, the cell monolayer was washed three times using blank Hanks' balanced salt solution (pH 7.4). The transepithelial electrical resistance values of cell monolayers were measured, and these values were greater than 300 Ωcm.[24] The monolayer was incubated with blank Hanks' balanced salt solution (pH 7.4) for 30 minutes at 37°C; subsequently, the incubation medium was aspirated. Next, a solution containing baohuoside I was loaded onto the apical or basolateral side of the monolayer. The amounts of transported baohuoside I were measured as a function of time by ultraperformance liquid chromatography (see below). Donor samples (400 µL) and receiver samples (400 µL) were taken at different times in triplicate, and 400 µL of the drug donor solution was added to the donor side or 400 µL of blank buffer was added to the receiver side. When comparing the permeability of baohuoside I and its phospholipid complex, each agent was used at the same concentration (10 µM) and samples were taken hours 0, 1, 2, 3, and 4 after incubation. To each transport sample (400 µL), 100 µL of acetonitrile containing genistein was added as an internal standard and preservative. The resulting mixtures were vortexed for 30 seconds and centrifuged at 15,000 rpm for 15 minutes. The supernatant was analyzed by ultraperformance liquid chromatography within 24 hours. At the end of the transport experiment, the integrity of the monolayer was examined by measuring its transepithelial electrical resistance value.[25]

Pharmacokinetic studies

Male rats were divided randomly into five groups for administration of a single dose of baohuoside I or baohuoside I-phospholipid complexes of different sizes. The five groups of rats were administered oral doses equivalent to 50 mg/kg of baohuoside I. To determine the serum drug concentrations and calculate the pharmacokinetic parameters, blood samples were collected at 0, 5, 15, 30, 45, 60, 90, 120, 240, 360, 480, and 720 minutes after dosing. The blood samples were centrifuged at 3000 rpm for 10 minutes, and the supernatants were collected into tightly sealed plastic tubes (containing a heparin sodium anticoagulation solution). We added 100 µL of an internal standard working solution (50 ng/mL carbamazepine in acetonitrile) to 100 µL of the plasma sample, and 900 µL of acetonitrile was then added to the mixture and vortexed for 30 seconds to precipitate the protein. The resulting mixture was centrifuged at 13,000 rpm

for 15 minutes at 4°C. One milliliter of the upper organic phase was transferred to another tube and evaporated to dryness at 25°C using a Thermo Savant SPD 2010 Speed Vac System (Thermo Electron Corporation, Waltham, MA). The residue was dissolved in 100 μL of methanol and vortex-mixed for one minute. After centrifugation at 15,000 rpm for 15 minutes, 40 μL of the supernatant was injected into a high-performance liquid chromatography-mass spectrometry system for analysis.

Analytical methods

For high-performance liquid chromatography analysis, a Zorbax SB-C18 column (4.6 × 250 mm, 5 μm) was used for the stationary phase and kept at 30°C. The mobile phase was a mixture of acetonitrile and water (75:25), and the flow rate was 1.0 mL per minute. Separation was monitored at 270 nm. The diode array detector acquisition wavelength was set at 200–400 nm.

Ultraperformance liquid chromatography was used to detect baohuoside I in the transport samples obtained in the Caco-2 model. The conditions for ultraperformance liquid chromatography analysis of baohuoside I in the transport samples and the baohuoside I-phospholipid complex samples were as follows: system, Waters Acquity ultraperformance liquid chromatography with a photodiode array detector and Empower software (Waters, Milford, MA); column, Acquity ultraperformance liquid chromatography BEH C18, 1.7 μm, 2.1 × 50 mm (Waters); mobile phase A, acetonitrile; mobile phase B, water containing 0.1% AcH; gradient, 0–0.9 minute, 25% A, 0.9–1 minute, 25%–60% A, 1–2 minutes, 60% A, 2–2.5 minutes, 60%–25% A, 2.5–3 minutes, 25% A; flow rate, 0.4 mL per minute; column temperature, 35°C; wavelength, 270 nm; and injection volume, 6 μL. The retention time for baohuoside I was 1.41 minutes. The retention time for genistein (the internal standard) was 1.54 minutes.

The mass spectrometer was operated in positive ionization mode using SCAN to measure baohuoside I at m/z 515.76–369.87, 28.80 minutes, and internal standard (carbamazepine) at m/z 237–194, 21.90 minutes. The voltages of the capillary and cone were 3 kV and 25 V, respectively. The flow rate of the heated drying gas was 350 L/hour, and the source temperature was 120°C. The temperature of the supplementary gas was 40°C. The structure was elucidated using electrospray ionization mass spectrometry at full scan from m/z 100–900. The stationary phase, mobile phase A, water contained 0.05% HCOOH; B, acetonitrile contained 0.05% HCOOH, gradient, 0–3 minutes, 95% A, 3–5 minutes, 95%–75% A, 5–18 minutes, 75% A, 18–40 minutes,

75%–10% A. A Zorbax SB-C18 column (4.6 × 250 mm, 5 μm) was used and kept at 30°C. The flow rate was 1.0 mL per minute. Separation was monitored at 270 nm.

Data analysis

The rate of transport was obtained from the amount transported versus the time curve using linear regression. The permeability of baohuoside I was calculated using the following equation:[20]

$$P_{app} = \frac{V}{S \times C} \times \frac{dC}{dt} = \frac{1}{S \times C} \times \frac{dM}{dt} \quad (1)$$

where V is the volume of the receiver (typical volume 2.5 mL), S is the surface area of the cell monolayer (typical surface area 4.2 cm^2), C is the initial concentration, dC/dt is the rate of concentration change on the receiver side, and dM/dt is the rate of drug transport. The rate of drug transport was obtained by linear regression analysis.

Statistical analysis

All experiments were performed at least in triplicate. Data are presented as the mean ± standard deviation. The data were analyzed by Student's t-test. A two-tailed t-test (Microsoft Excel®) was used to identify significant differences ($P < 0.05$) compared with the controls.

Results and discussion

Sizing of nanoscale phospholipid complexes

The phospholipid complexes were efficiently dispersed during the homogenization procedure (Table 1). After homogenization, the mean diameter of the particles was reduced. The increased energy input resulted in efficient reduction of the particle size with an increase in homogenization pressure. However, varying the number of homogenization cycles from three to five had no significant effect on the particle size. Under the homogenization conditions, phospholipid

Table 1 Physicochemical properties of the baohuoside I-phospholipid complex (n = 3)

	Average size	Zeta potential
Baohuoside I-phospholipid complex (a)	227.3 ± 65.2 μm	
Baohuoside I-phospholipid complex (b)	262 ± 24 nm	−18.9 ± 4.9 mV
Baohuoside I-phospholipid complex (c)	148 ± 12 nm	−19.7 ± 3.3 mV
Baohuoside I-phospholipid complex (d)	81 ± 10 nm	−17.4 ± 4.7 mV

complexes of different sizes and zeta potentials were detected (Table 1). We obtained baohuoside I-phospholipid complexes with ideal particle size properties, and transmission electron microscopy revealed their morphological characteristics as black oval spheres (Figure 2).

Ultraviolet spectroscopy

Baohuoside I and nanoscale 81 ± 10 nm baohuoside I-phospholipid complexes were dissolved in ethanol and assayed using high-performance liquid chromatography. These two agents had the same retention times and ultraviolet absorption characteristics, suggesting that the structure of baohuoside I had not changed after its conversion to the phospholipid form (Figures 3 and 4).

Differential scanning calorimetry

The differential scanning calorimetry curves for baohuoside I, the phospholipids, the physical mixture, and nanoscale 81 ± 10 nm baohuoside I-phospholipid complexes are shown in Figure 5. The thermogram of baohuoside I shows that the main endothermic peak was at 168.3°C. However, the phospholipids clearly exhibit two different types of endothermic peaks. The first peak at 127.1°C was mild, which suggests that it had formed because of hot movements of the polar part of the phospholipid molecule. The second endothermic peak (364.8°C) was sharp and could have formed because of the phase transition from a gel-like state to a liquid crystal state, and the carbon-chain in the phospholipids may have undergone melting or isomeric or crystal changes.[26] Differential scanning calorimetry thermograms of the physical mixture of baohuoside I and the phospholipids showed two peaks. The former peak appeared at the

same onset temperature as that of baohuoside I (169.1°C), and the latter peak appeared at the same onset temperature as that of the complex (392.5°C). It might be assumed that the phospholipids melted with an increase in temperature, which caused baohuoside I to dissolve in the phospholipids, partly forming the complex.[27–29] The differential scanning calorimetry thermograms of the nanoscale 81 ± 10 nm phospholipid complex showed that the endothermic peak of the drug had disappeared. Instead, there was a new peak (391.8°C), possibly due to interactions between baohuoside I and the phospholipids, such as a combination of hydrogen bonds or van der Waals forces.

Transport of baohuoside I ± phospholipid complexes across Caco-2 cell monolayer

We assessed the permeability of the baohuoside I-phospholipid complexes using the Caco-2 monolayer and compared them with those of free baohuoside I. The nanoscale baohuoside I-phospholipid complexes of different sizes (262 ± 24 nm, 148 ± 12 nm, and 81 ± 10 nm) significantly ($P < 0.05$) increased the absorptive permeability of baohuoside I (Figure 6). The absorptive permeability of the 262 ± 24 nm, 148 ± 12 nm, and 81 ± 10 nm complexes showed increases of 122%, 212%, and 280%, respectively, compared with those of the control free baohuoside I. Likewise, the secretory permeability of baohuoside I was also significantly ($P < 0.05$) increased, showing increases of 75%, 140%, and 189%, respectively. This indicates that reduction in the size of the nanoscale baohuoside I-phospholipid complex promoted absorption and efflux, although it had no significant effect on the efflux ratio. Compared with baohuoside I, the nanoscale baohuoside I-phospholipid complexes promoted absorption.
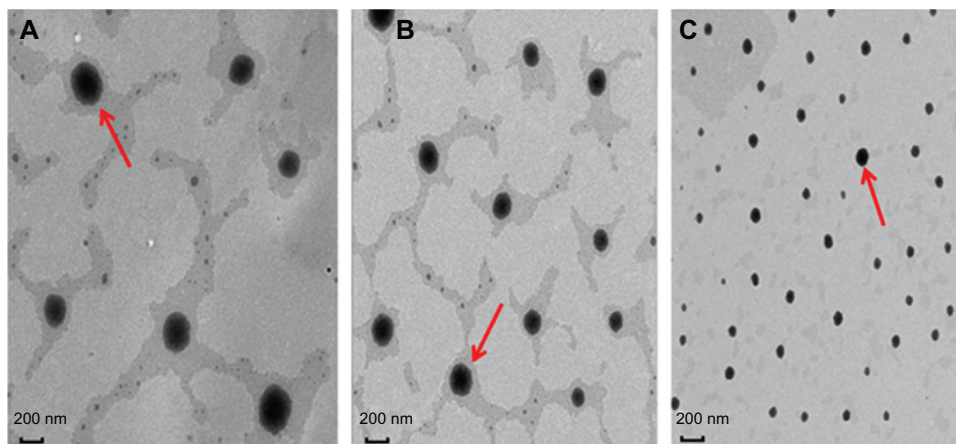

Figure 2 Transmission electron microscopic images of baohuoside I-phospholipid complexes of different sizes. (**A**) 262 ± 24 nm, (**B**) 148 ± 12 nm, and (**C**) 81 ± 10 nm.
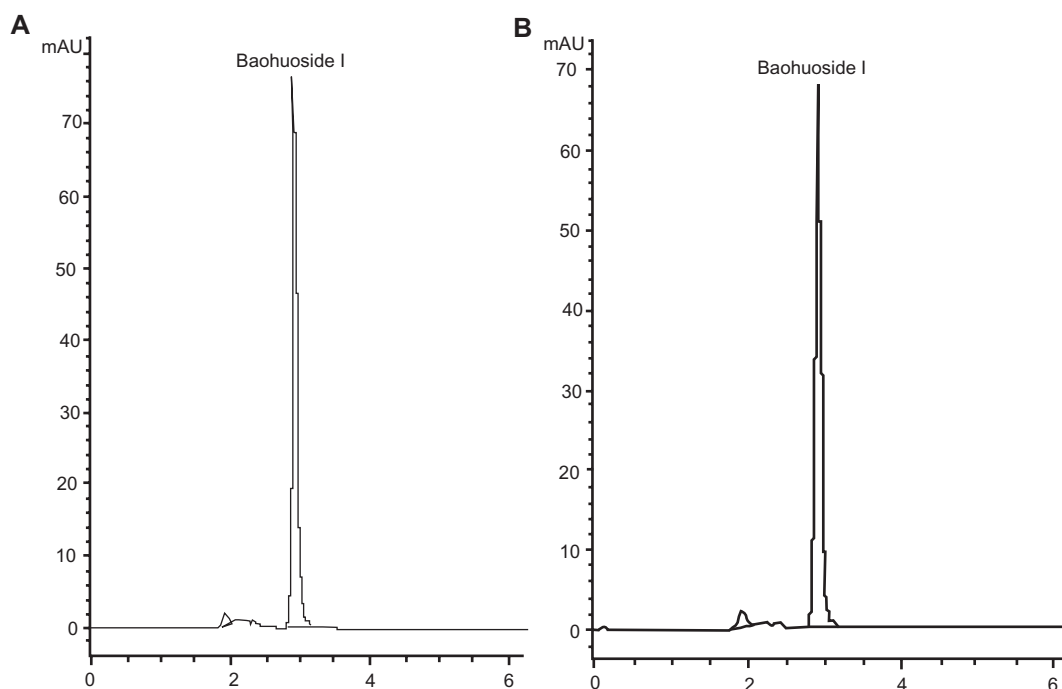
Figure 3 Chromatograms of (**A**) baohuoside I and (**B**) a nanoscale baohuoside I-phospholipid complex (81 ± 10 nm).

This was mainly because of the phospholipid characteristics of the complex, which included interaction with the lipid bilayer, leading to increased membrane permeability.

Baohuoside I had a higher efflux ratio (7.76, calculated on the basis of the formulations prepared at pH 7.4 after 4 hours) than the nanoscale baohuoside I-phospholipid complexes (6.12 for the 262 ± 24 nm complex, 5.98 for the 148 ± 12 nm complex, and 5.91 for the 81 ± 10 nm complex). Thus, it can be inferred that absorption of the nanoscale baohuoside I-phospholipid complexes was greater than that of the baohuoside I. Additionally, the

efflux ratio of baohuoside I decreased significantly after formation of nanoscale baohuoside I-phospholipid complexes (Table 2).

Pharmacokinetics of baohuoside I and its phospholipid complexes after oral dosing

We assessed the oral bioavailability of the baohuoside I-phospholipid complexes in rats and compared it with that of baohuoside I. The mean baohuoside I plasma concentration versus time plots for five samples equivalent to 50 mg/kg doses of baohuoside I orally administered to rats (n = 6) are
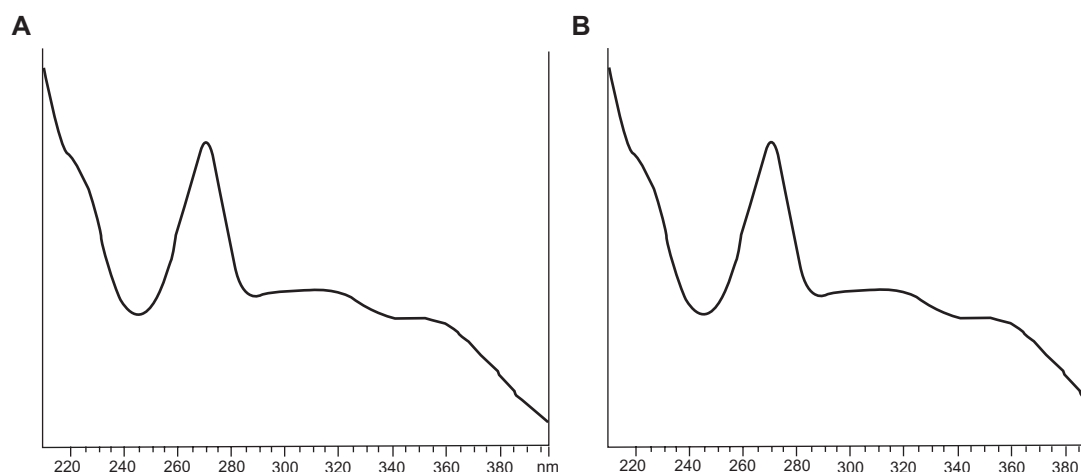

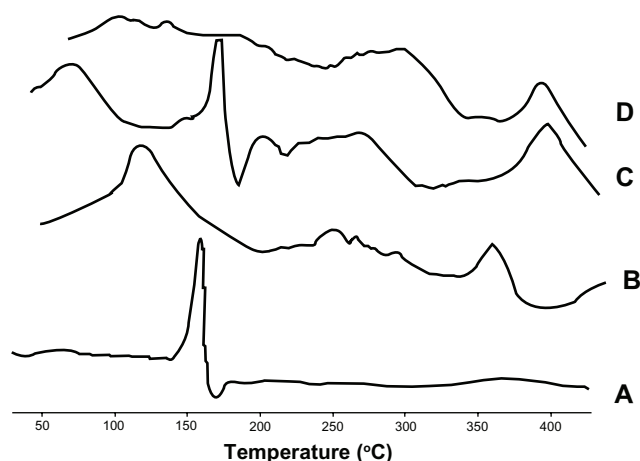**Figure 4** Ultraviolet spectra of (**A**) baohuoside I and (**B**) a nanoscale baohuoside I-phospholipid complex (81 ± 10 nm).

Figure 5 Differential scanning calorimetry thermograms of (**A**) baohuoside I, (**B**) the phospholipids, (**C**) the physical mixture, and (**D**) the nanoscale baohuoside I-phospholipid complex.

Table 2 Permeabilities (P_{app}) and efflux ratios of baohuoside I and the nanoscale baohuoside I-phospholipid complex

Compound	$P_{app} \times 10^{-6}$ (cm/sec)		Efflux ratio
	A − B	**B − A**	
Baohuoside I	1.85 ± 0.18	14.36 ± 0.72	7.76
Baohuoside I-phospholipid complex (262 ± 24 nm)	4.12 ± 0.34*	25.21 ± 1.49*	6.12*
Baohuoside I-phospholipid complex (148 ± 12 nm)	5.78 ± 0.86*	34.56 ± 3.77*	5.98*
Baohuoside I-phospholipid complex (81 ± 10 nm)	7.03 ± 0.96*	41.55 ± 3.53*	5.91*

Notes: The absorptive permeability was expressed as A − B, whereas the secretory permeability was expressed as B − A. The efflux ratio was P_{app} (B − A)/P_{app} (A − B). Data are presented as the mean ± standard deviation; n = 3; *$P < 0.05$ versus the baohuoside I group.

shown in Figure 7. A summary of the statistical analysis is shown in Table 3. The average values for maximum concentration and time to maximum concentration after oral administration of baohuoside I were 296.32 ng/mL and 50 minutes, respectively, while those after oral administration of the 227.3 ± 65.2 µm baohuoside I-phospholipid complex were 525.37 ng/mL and 52.5 minutes, respectively. The average $AUC_{0-\infty}$ of the 227.3 ± 65.2 µm baohuoside I-phospholipid complex in rats was 146.98 mg · min/L, which was significantly higher than that of the free baohuoside I. The $AUC_{0-\infty}$ of the 227.3 ± 65.2 µm baohuoside I-phospholipid complex was 2.08 times greater than that of free baohuoside I.

The relative bioavailability of baohuoside I increased with a decrease in the size of the baohuoside I-phospholipid
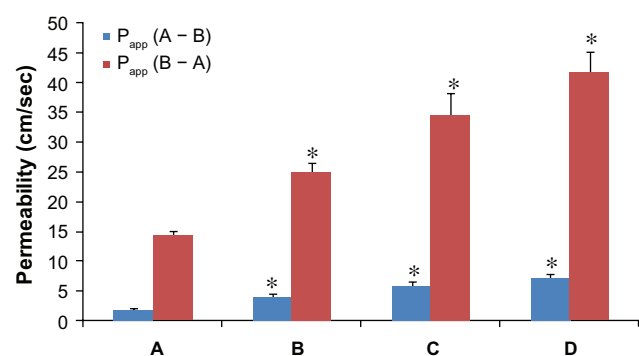

Figure 6 Permeability of (**A**) baohuoside I, (**B**) the baohuoside I-phospholipid complex of 262 ± 24 nm, (**C**) the baohuoside I-phospholipid complex of 148 ± 12 nm, and (**D**) the baohuoside I-phospholipid complex of 81 ± 10 nm.
Notes: The rates of transport were used to calculate the absorptive permeability [P_{app} (A − B)] and secretory permeability [P_{app} (B − A)] using Equation (1), and the calculated permeabilities are plotted here as bars. The data are expressed as the mean ± standard deviation (n = 3). *$P < 0.05$ baohuoside I versus the baohuoside I-phospholipid complex, with more asterisks indicating higher levels of significance (one-way analysis of variance followed by Tamhane's post hoc test).

complex. Interestingly, the time to maximum concentration values of the nanoscale baohuoside I-phospholipid complexes (262 ± 24 nm, 148 ± 12 nm, and 81 ± 10 nm) significantly decreased with a reduction in particle size. Furthermore, the relative bioavailability of the nanoscale 81 ± 10 nm baohuoside I-phospholipid complex ($AUC_{0-\infty}$) was 342% compared with 165% for baohuoside I ($AUC_{0-\infty}$) and the common 227.3 ± 65.2 µm baohuoside I-phospholipid complex ($AUC_{0-\infty}$).

Flavonoids are the most important phytochemicals that modify the natural biological response because of their antiviral, anticancerous, and antiallergic properties, but they have poor or very poor absorption after oral administration. The poor absorption of flavonoids is mainly due to low membrane permeability, poor aqueous solubility, or bacterial degradation in the gastrointestinal tract.[30]

Phospholipid complexes, which are usually formed in nonaqueous solvents, have been studied for many years for their ability to enhance the oral bioavailability of drugs with poor oral absorption.[31–34] Phospholipid complexes as nanocarriers have many advantages because they are formed from biocompatible, biodegradable, and relatively nontoxic molecules. However, to the best of our knowledge, no studies have reported the influence of nanoscale phospholipid complexes on absorption. Therefore, we attempted to evaluate the influence of phospholipid complexes of different diameters on the oral absorption of baohuoside I in vitro and in vivo. Our results suggest that the smaller the size of the particles, the faster they cross a Caco-2 monolayer, and the faster they are resorbed after oral administration in rats.

Therefore, use of nanoscale phospholipid complexes can effectively enhance the absorption of baohuoside I in vitro and also dramatically improve its bioavailability in vivo. The
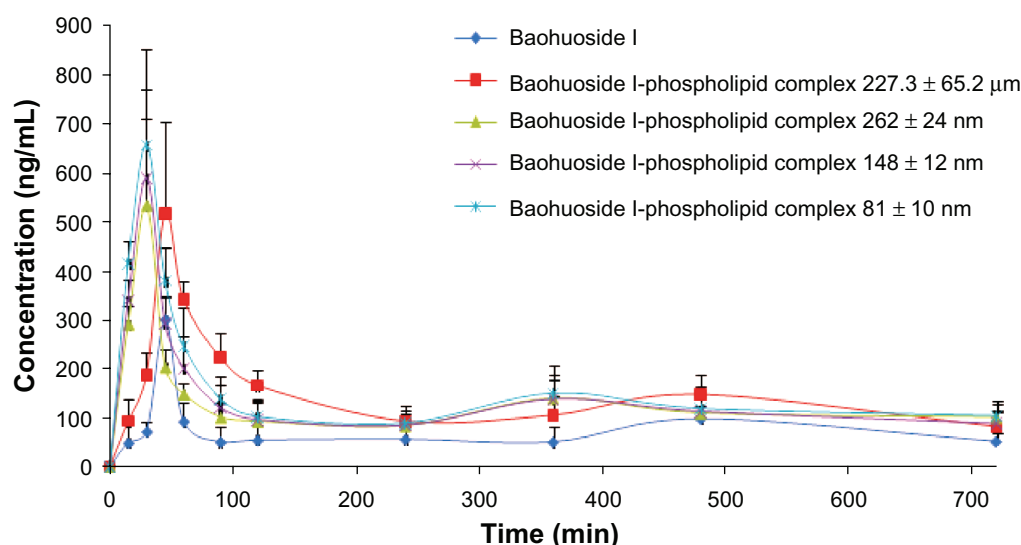
Figure 7 Plasma concentration-time curve in rats after oral administration of baohuoside I and the baohuoside I-phospholipid complexes of 227.3 ± 65.2 μm, 262 ± 24 nm, 148 ± 12 nm, and 81 ± 10 nm.
Notes: The baohuoside I dose was 50 mg/kg. The data are presented as the mean ± standard deviation (n = 6).

nanoscale phospholipid complex may improve the absorption of baohuoside I as follows. After formation of the phospholipid complex, with the decrease in particle size, the complex is more effectively combined with the cell membrane, which consists of phospholipids. Thus, we decreased the size of the phospholipid complex as well as increased its specific surface area and fluidity. The nanoscale phospholipid complex had a significant effect on the specific region of the gastrointestinal tract where the drug is absorbed.[35–37] Some studies have suggested that intestinal mucosal cell delivery can be facilitated by restricting the delivery vehicles to the nanometer size range.

Peyer's patches, which are nodules of lymphatic cells that aggregate to form bundles or patches and occur usually only in the lowest portion (ileum) of the small intestine, are named after the 17th century Swiss anatomist, Hans Conrad Peyer. Peyer's patches are round or oval, and are located in the mucous membrane lining the intestine. They can be seen by the naked eye as elongated thickened areas, and their surface is free of the projections (villi) and depressions (Lieberkühn glands) characteristic of the intestinal wall. Usually an individual has only 30–40 patches, which account for 25% of intestinal mucosal cells. Nanoparticles have an increased uptake in Peyer's patches. In the Peyer's patches, particles with an average diameter of 100 nm are absorbed more easily than other particles.[38] Therefore, we enhanced the oral bioavailability of baohuoside I by decreasing the particle size of the phospholipid complex into the nanometer range, which improved the potential of baohuoside I for clinical application. To date, few studies have described the absorption mechanism and transport processes of phospholipid complexes. Therefore, further studies are required to address this issue.

Table 3 Pharmacokinetic parameters of baohuoside I, baohuoside I-phospholipid complex of 227.3 ± 65.2 μm (BPC a), baohuoside I-phospholipid complex of 262 ± 24 nm (BPC b), baohuoside I-phospholipid complex of 148 ± 12 nm (BPC c), and baohuoside I-phospholipid complex of 81 ± 10 nm (BPC d) 50 mg/kg, orally in rats (n = 6)

Parameters	Baohuoside I	BPC a	BPC b	BPC c	BPC d
AUC_{0-t} (mg · min/L)	65.21 ± 12.29	114.37 ± 20.28*	131.39 ± 31.29*,#	154.34 ± 35.29*,#	186.81 ± 44.32*,#
$AUC_{0-\infty}$ (mg · min/L)	70.65 ± 14.16	146.98 ± 21.96*	179.75 ± 28.72*,#	193.84 ± 37.51*,#	242.09 ± 52.19*,#
MRT_{0-t} (min)	471.33 ± 51.43	491.21 ± 72.14	521.49 ± 89.19	571.92 ± 98.64	641.94 ± 109.24*,#
$MRT_{0-\infty}$ (min)	569.58 ± 51.94	598.77 ± 68.53	659.44 ± 89.08	674.21 ± 100.23	763.78 ± 135.38*,#
T_{max} (min)	53.71 ± 7.75	55.65 ± 8.22	37.32 ± 10.28*,#	32.58 ± 9.56*,#	27.13 ± 7.41*,#
C_{max} (ng/mL)	296.32 ± 31.38	525.37 ± 69.45*	552.15 ± 89.92*	587.48 ± 89.92*,#	654.87 ± 89.92*,#

Notes: The data are presented as the mean ± standard deviation. *$P < 0.05$ versus 50 mg/kg baohuoside I; #$P < 0.05$, versus baohuoside I-phospholipid complex of 227.3 ± 65.2 μm, which contained baohuoside I 50 mg/kg.
Abbreviations: AUC, area under concentration-time curve; MRT, mean residence time; T_{max}, time to maximum plasma concentration; C_{max}, maximum plasma concentration.

Conclusion

The results of our study show that the nanoscale phospholipid complex was superior to the common phospholipid complex in improving the oral bioavailability of baohuoside I. In addition, our results indicate that particles of a smaller size improve the oral absorption of baohuoside I.

Acknowledgments

Disclosure

The authors report no conflicts of interest in this work.

References

1. Qian Q, Li SL, Sun E, et al. Metabolite profiles of icariin in rat plasma by ultra-fast liquid chromatography coupled to triple-quadrupole/time-of-flight mass spectrometry. *J Pharm Biomed Anal*. 2012;66:392–398.
2. Lee KS, Lee HJ, Kwang SA, et al. Cyclooxygenase-2/prostaglandin E2 pathway mediates icariside II induced apoptosis in human PC-3 prostate cancer cells. *Cancer Lett*. 2009;1:93–100.
3. Kim SH, Kwang SA, Jeong SJ, et al. Janus activated kinase 2/signal transducer and activator of transcription 3 pathway mediates icariside II-induced apoptosis in U266 multiple myeloma cells. *Eur J Pharmacol*. 2011;1:10–16.
4. Choi HJ, Eun JS, Kim DK, et al. Icariside II from Epimedium koreanum inhibits hypoxia-inducible factor-1α in human osteosarcoma cells. *Eur J Pharmacol*. 2008;579:58–65.
5. Jeong EJ, Liu X, Jia X, et al. Coupling of conjugating enzymes and efflux transporters: impact on bioavailability and drug interactions. *Curr Drug Metab*. 2005;6:455–468.
6. Xiao YY, Song YM, Chen ZP, et al. The preparation of silybin-phospholipid complex and the study on its pharmacokinetics in rats. *Int J Pharm*. 2006;307:77–82.
7. Chen ZP, Sun J, Chen HX, et al. Comparative pharmacokinetics and bioavailability studies of quercetin, kaempferol and isorhamnetin after oral administration of *Ginkgo biloba* extracts, *Ginkgo biloba* extract phospholipid complexes and *Ginkgo biloba* extract solid dispersions in rats. *Fitoterapia*. 2010;81:1045–1052.
8. Zhang JJ, Peng Q, Shi SJ, et al. Preparation, characterization, and in vivo evaluation of a self-nanoemulsifying drug delivery system (SNEDDs) loaded with morin-phospholipid complex. *Int J Nanomedicine*. 2011;6:3405–3414.
9. Kuntal MT, Kakali M, Arunava G, et al. Curcumin-phospholipid complex: preparation, therapeutic evaluation and pharmacokinetic study in rats. *Int J Pharm*. 2007;330:155–163.
10. Yan L, Zhang Y, Yang ZY, et al. Formulation of an intravenous emulsion loaded with a clarithromycin-phospholipid complex and its pharmacokinetics in rats. *Int J Pharm*. 2009;366:160–169.
11. Morazzoni P, Montalbetti A, Malandrino S, et al. Comparative pharmacokinetics of silybin-phosphatidylcholine complex and silymarin in rats. *Eur J Drug Metab Pharmacokinet*. 1993;18:289–297.
12. Ilie I, Ilie R, Mocan T, et al. Influence of nanomaterials on stem cell differentiation: designing an appropriate nanobiointerface. *Int J Nanomedicine*. 2012;7:2211–2225.
13. Ranganathan R, Madanmohan S, Kesavan A, et al. Nanomedicine: towards development of patient-friendly drug-delivery systems for oncological applications. *Int J Nanomedicine*. 2012;7:1043–1060.
14. Siddiqui IA, Adhami VM, Christopher J, et al. Impact of nanotechnology in cancer: emphasis on nanochemoprevention. *Int J Nanomedicine*. 2012;7:591–605.
15. Kutikhin AG, Brusina EB, Yuzhalin AE. The role of calcifying nanoparticles in biology and medicine. *Int J Nanomedicine*. 2012;7:339–350.
16. Coyuco JC, Liu YJ, Tan BJ, et al. Functionalized carbon nanomaterials: exploring the interactions with Caco-2 cells for potential oral drug delivery. *Int J Nanomedicine*. 2011;6:2253–2263.
17. Guan M, Zhu QL, Liu Y, et al. Uptake and transport of a novel anticancer drug-delivery system: lactosyl-norcantharidin-associated N-trimethyl chitosan nanoparticles across intestinal Caco-2 cell monolayers. *Int J Nanomedicine*. 2012;7:1921–1930.
18. Caro I, Boulenc X, Rousset M, et al. Characterisation of a newly isolated Caco-2clone (TC-7), as a model of transport processes and biotransformation of drugs. *Int J Pharm*. 1995;116:147–158.
19. Jin X, Zhang ZH, Sun ET, et al. Preparation of icariside II-phospholipid complex and its absorption across Caco-2 cell monolayers. *Pharmazie*. 2012;67:293–298.
20. Hu M, Chen J, Zhu Y, et al. Mechanism and kinetics of transcellular transport of a new beta-lactam antibiotic loracarbef across an intestinal epithelial membrane model system (Caco-2). *Pharm Res*. 1994;11:1405–1413.
21. Jia XB, Chen J, Lin H, et al. Disposition of flavonoids via enteric recycling: enzyme-transporter coupling affects metabolism of biochanin A and formononetin and excretion of their phase II conjugates. *J Pharmacol Exp Ther*. 2004;310:1103–1113.
22. Hu M, Chen J, Lin H. Metabolism of flavonoids via enteric recycling: mechanistic studies of diposition of apigenin in theCaco-2 cell culture model. *J Pharmacol Exp Ther*. 2003;307:314–321.
23. Karamustafa F. Transport of alendronate through human intestinal cell line, Caco-2. *33rd Annual Meeting and Exposition of the Controlled Release Society*. 2006;7:22–26.
24. Roger E, Lagarce F, Garcion E, et al. Lipid nanocarriers improve paclitaxel transport throughout human intestinal epithelial cells by using vesicle-mediated transcytosis. *J Control Release*. 2009;140:174–181.
25. Lev B, Valery A. Effects of polyether-modified poly (acrylic acid) microgels on doxorubicin transport in human intestinal epithelial Caco-2 cell. *J Control Release*. 2003;88:11–22.
26. Maiti K, Mukhefjee K, Gantait A, et al. Curcumin-phospholipid complex: preparation, therapeutic evaluation and pharmacokinetic study in rats. *Int J Pharm*. 2007;330:55–63.
27. Hüsch J, Dutagaci B, Glaubitz C, et al. Structural properties of the so-called NSAID–phospholipid-complexes. *Eur J Pharm Sci*. 2011;44:103–116.
28. Parmar KF, Satapara VP, Shah SR, et al. Improvement of dissolution properties of lamotrigine by inclusion complexation and solid dispersion technique. *Pharmazie*. 2011;66:119–123.
29. Ruan JH, Liua J, Zhu D, et al. Preparation and evaluation of self-nanoemulsified drug delivery systems (SNEDDSs) of matrine based on drug–phospholipid complex technique. *Int J Pharm*. 2010;386:282–290.
30. Bruneton J. *Pharmacognosy Phytochemistry Medicinal Plants*. Paris, France: Lavoisier Publication; 1999.
31. Liu AC, Lou HX, Zhao LX, et al. Validated LC/MS/MS assay for curcumin and tetrahydrocurcumin in rat plasma and application to pharmacokinetic study of phospholipid complex of curcumin. *J Pharm Biomed Anal*. 2006;40:720–727.
32. Yue PF, Yuan HL, Li XY, et al. Process optimization, characterization and evaluation in vivo of oxymatrine-phospholipid complex. *Int J Pharm*. 2010;387:139–146.
33. Maiti K, Mukherjee K, et al. Enhanced therapeutic benefit of quercetin-phospholipid complex in carbon tetrachloride induced acute liver injury in rats: a comparative study. *Iran J Pharmacol Ther*. 2005;4:84–90.

34. Rahila AP, Uma B. Gymnemic acid-phospholipid complex: preparation and characterization. *J Dispers Sci Technol*. 2011;32:1165–1172.

35. Pukanud P, Peungvicha P, Sarisuta N. Development of mannosylated liposomes for bioadhesive oral drug delivery via M cells of Peyer's patches. *Drug Deliv*. 2009;16:289–294.

36. Ermak T, Giannasca PJ. Microparticle targeting to M cells. *Adv Drug Deliv Rev*. 1998;34:261–283.

37. Borges O, Borchard G, Verhoef JC, et al. Preparation of coated nanoparticles for a new mucosal vaccine delivery system. *Int J Pharm*. 2005;299:155–166.

38. Desai MP, Labhasetwar V, Amidon GL, et al. Gastrointestinal uptake of biodegradable microparticles: effect of particle size. *Pharm Res*. 1996;13:1838–1845.